A Photonic Temporal Integrator With an Ultra-Long Integration Time Window Based on an InP-InGaAsP Integrated Ring Resonator

Weilin Liu, *Student Member, IEEE*, Ming Li, *Member, IEEE*, Robert S. Guzzon, Erik J. Norberg, John S. Parker, Larry A. Coldren, *Life Fellow, IEEE, Fellow, OSA*, and Jianping Yao, *Fellow, IEEE, Fellow, OSA*

***Abstract*—A photonic temporal integrator with an ultra-wide integration time window implemented based on a photonic integrated circuit (PIC) in an InP-InGaAsP material system consisting of semiconductor optical amplifiers (SOAs) and current-injection phase modulators (PMs) is proposed and experimentally demonstrated. The proposed photonic integrated integrator employs a ring structure coupled with two bypass waveguides. The tunable coupling between the ring and the waveguides is realized by a multimode interference (MMI) Mach-Zehnder interferometer coupler. Within the ring, two SOAs are incorporated to compensate for the insertion loss. In addition, there is a current injection PM in the ring for wavelength tuning. The use of the device provides a photonic temporal integrator with an ultra-wide integration time window and a tunable operation wavelength in a single PIC. The proposed integrator is fabricated and experimentally verified. The integration time window as wide as 6331 ps is achieved, which is an order of magnitude longer than that provided by the previously reported photonic integrators.**

***Index Terms*—Analog optical signal processing, photonic integrated circuits (PICs), temporal integrator, ultrafast processing.**

I. Introduction

A PHOTONIC temporal integrator, which performs the time integral of an input signal, is an important device for data processing [1], optical memory [2], and optical computing [3], [4]. A photonic temporal integrator, as a fundamental building block for all-optical signal processing, overcomes the speed limitation of its electronic counterparts. In the last few years, the implementation of a temporal integrator based on photonic techniques has been widely investigated, such as the implementation using a fiber Bragg grating (FBG) [5]–[9] or a microring resonator [10], [11]. In [5], Asghari and Azaña introduced a single uniform FBG incorporating phase shifts along its axial profile to realize an all-optical arbitrary-order temporal integrator. By simply propagating an input optical waveform through the FBG, the cumulative time integral of the complex field envelope of the input waveform can be obtained. The proposed integrator was investigated numerically and optimized by maximizing its power efficiency [6], and a second-order complex-field temporal integrator was experimentally demonstrated with a single apodized uniform-period FBG [7], [8]. To compensate for the insertion loss in the FBG, Slavík *et al.* proposed an all-optical gain-assisted temporal integrator based on a superimposed FBG made in an Er-Yb co-doped optical fiber [9]. A photonic temporal integrator was experimentally demonstrated using the active resonant cavity in the superimposed FBG operating at the exact lasing threshold condition. In these approaches, although the main component is an FBG, the implementation of the system needs multiple discrete components, which makes the system bulky. In addition, the system cannot be reconfigured once the FBG is fabricated. To solve the problems, Ferrera *et al.* proposed an on-chip CMOS-compatible all-optical integrator [10]. The key component in the integrator is a passive micro-ring resonator. The 1st-order temporal integration of a complex-field optical waveform, with a time resolution of ~8 ps over an integration window exceeding 800 ps, was achieved. However, the throughput of the device was reduced by its very narrow resonance linewidth. The tradeoff between the integration bandwidth and overall power efficiency by performing all-optical integration in a micro ring resonator was explored [11]. An input to output power efficiency of 1.5% and an integration time window of ~12.5 ps was achieved.

Recently, we proposed a chip-scale photonic temporal integrator in an InP-InGaAsP material system with an ultra-high power efficiency by incorporating semiconductor optical amplifiers (SOAs) and current injection phase modulators (PMs) in a micro-ring resonator [12]. The photonic temporal integrator employs a ring structure coupled with two bypass waveguides. The coupling coefficients between the ring and waveguides are tunable, which is realized by a multi-mode interference (MMI) Mach-Zehnder interferometer (MZI) coupler. Within the ring, there are two SOAs providing a peak gain of 9.6 dB per SOA to compensate for a total insertion loss of 3.6 dB. In addition, there is a current injection PM in the ring for wavelength tuning. The use of the device provides, for the first time to the best of our knowledge, a photonic temporal integrator with both ultra-long integration time and tunable operation wavelength in a single photonic integrated circuit (PIC).

Manuscript received January 14, 2014; revised April 14, 2014; accepted March 14, 2014. Date of publication May 12, 2014; date of current version September 1, 2014. This work was supported by the Natural Science and Engineering Research Council of Canada.

W. Liu and J. Yao are with the Microwave Photonics Research Laboratory, School of Electrical Engineering and Computer Science, University of Ottawa, ON K1N 6N5, Canada (e-mail: wliu020@uottawa.ca; jpyao@eecs.uOttawa.ca).

M. Li is with the Institute of Semiconductors, Chinese Academy of Sciences, Beijing 100044, China (e-mail: ml@semi.ac.cn).

R. S. Guzzon, E. J. Norberg, J. S. Parker, and L. A. Coldren are with the Department of Electrical and Computer Engineering, University of California Santa Barbara, Santa Barbara, CA 93116 USA (e-mail: rob.guzzon@gmail.com; norberg@ece.ucsb.edu; jjsparker@gmail.com; coldren@ece.ucsb.edu).

Color versions of one or more of the figures in this paper are available online at http://ieeexplore.ieee.org.

Digital Object Identifier 10.1109/JLT.2014.2323249

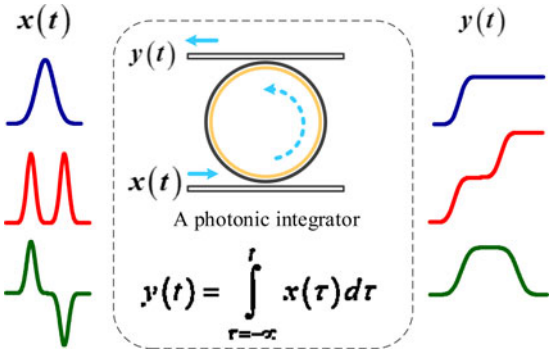

Fig. 1. The schematic diagram of a photonic temporal integrator based on a microring resonator.

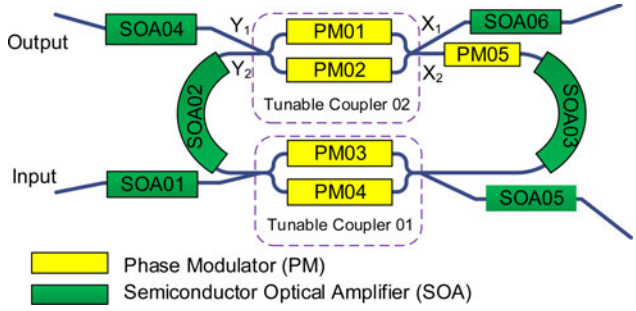

Fig. 2. The schematic of the proposed on-chip photonic temporal integrator based on a microring resonator.

The photonic temporal integrator proposed in [12] can be configured with a much larger integration time window for photonic temporal integration. In this paper, we provide a detailed theoretical study of the active temporal integrator reported in [12] and demonstrate the operation of the integrator with significantly improved performance. By optimizing the currents applied to the active components on the chip, the ring can be configured to work close to its lasing condition, at which, the integration time window can be significantly increased. In the experimental demonstration, the integration time window is improved from 198 to 6331 ps.

The paper is organized as follows. In Section II, the principle of the active temporal integrator is presented, with an emphasis on the configuration of the integrator to operate close to its lasing condition by tuning the injection currents to the SOAs on the chip to improve the integration time window. A simulation is then performed to study the integration time window for different Q-factors of the ring. In Section III, an experiment is performed. The temporal integration of a Gaussian shaped pulse, an in-phase doublet and an out-of-phase doublet pulse is demonstrated, with the integrated results measured and analyzed. The integration time window of the proposed integrator is measured to be 6331 ps. A conclusion is drawn in Section IV.

II. Principle

Mathematically, a temporal integrator can be implemented using a linear time-invariant filter with a transfer function given by [11]

$$H(\omega) = \frac{1}{j(\omega - \omega_0)} \tag{1}$$

where $j = \sqrt{-1}$, ω is the angular optical frequency and ω_0 is the carrier frequency of the signal to be processed. A general approach to realizing a photonic integrator is to use an optical resonant cavity, for example, a Fabry–Pérot filter [9] or a ring resonator [10]–[12]. Fig. 1 shows a photonic temporal integrator based on a microring resonator. Three output temporal waveforms corresponding to three input waveforms of a Gaussian pulse, an in-phase doublet, and an out-of-phase doublet are shown to demonstrate the integration operation. The detailed theoretical analysis of using a ring resonator to implement an optical integrator could be found in [13]. However, the integration time window of such an integrator is limited, and its operation wavelength is usually fixed. To implement a photonic integrator with an ultra-long integration time window and a tunable operation wavelength, we propose to use an active ring resonator incorporating SOAs and current injection PMs, as shown in Fig. 2.

The frequency response of the ring resonator in Fig. 2 consists of a series of narrow passbands with two neighboring passbands separated by a free spectral range (FSR) determined by the length of the ring [12]. By locating the central frequency of the input signal at the center of one of the narrow passband, the temporal integral of the input signal can be obtained at the output of the ring. In our design, to achieve temporal integration with an ultra-long integration time and a tunable working wavelength, two active SOAs (SOA02 and SOA03) and a current injection PM (PM05) are incorporated into the ring. By applying injection currents to the SOAs (SOA02 and SOA03), the insertion loss in the device can be totally compensated. By changing the injection current to the PM (PM05) in the ring resonator, the spectral response is laterally shifted, thus making the operating wavelength be tuned. In addition, the coupling between the ring and the bypass waveguides is achieved by two tunable couplers, with each having an MMI MZI structure consisting of one PM in each of the two arms (PM01 and PM02 for tunable coupler 01, and PM03 and PM04 for tunable coupler 02, as shown in Fig. 2). By changing the injection currents to the PMs in the tunable couplers, the coupling coefficients can be continuously tuned from 0% to 100%. To compensate for the fiber coupling losses, two other active SOAs (SOA01 and SOA04) are incorporated into the device at the input and output waveguides, respectively. In this way, a photonic temporal integrator with an ultra-high power efficiency and a continuously tunable operating wavelength can be achieved.

Theoretically, the transfer function of the proposed ring resonator with the output taken from the drop port shown in Fig. 2 is given by [14]

$$H(Z) = -\frac{\kappa_1 \kappa_2 \sqrt{\rho Z^{-1}}}{1 - t_1 t_2 \rho Z^{-1}} \tag{2}$$

where κ_1 and κ_2 are the field coupling coefficients of the two tunable couplers, t_1 and t_2 are the field transmission factors of

TABLE I
PARAMETERS FOR THE SIMULATION

Symbol	Description	Value
λ	Central wavelength	1558 nm
γ_1	Coupling coefficient of the input coupler	90% (0–100%)
γ_2	Coupling coefficient of the output coupler	90% (0–100%)
l	Length of the ring	3 mm
n	Refractive index of the waveguide	3.67
α	Waveguide loss	1.7 dB/cm
ρ	Insertion loss of the tunable coupler	2 dB
g	Gain of each SOA	0–9.6 dB

Coupler coefficients are tunable from 0% to 100%, which are considered as the coupling coefficient from X_2 to Y_2 as shown in Fig. 2.

the two tunable couplers, and ρ is the loss in the ring. If the insertion losses in the ring are completely compensated, the Q-factor of the ring is infinite, and the integration time is infinitely long. For real implementations, however, it is too difficult to achieve a complete compensation for the losses without reaching the lasing threshold ($t_1 t_2 \rho = 1$). Thus, we discuss the integration time window when the Q-factor of the ring is tuned by changing the injection currents to the SOAs on the chip, to achieve a large Q-factor while ensuring the ring is not lasing. The Q-factor of the ring is given by [15]

$$Q = \omega_r \frac{\mathrm{T}_r}{\alpha L} = \omega_r \mathrm{N} \mathrm{T}_r \tag{3}$$

where ω_r is the resonant angular frequency of the ring resonator, T_r is the round trip time in the ring, α is the power attenuation coefficient, L is the optical length of the ring, and N is the number of round trips required to reduce the optical power to $1/e$. The integration time window is defined as the time duration for the output power to drop by 20% from its maximum value [10]. A simulation is performed to analyze the integration performance for the ring to be configured to operate far from the lasing condition to close to the lasing condition. In the simulation, the integration time window is calculated based on the output temporal waveform, which is obtained by an inverse Fourier transform of the product of the input Gaussian pulse spectrum and the transfer function of the ring resonator with different Q-factors. The parameters in the simulation are given in Table I. As shown in Fig. 3, the integration time window increases with the Q-factor. When the ring is approaching to the lasing threshold or the Q-factor is approaching to infinity, the integration time window is then approaching to infinity. However, for practical implementation, the ring resonator is very unstable when the gain is close to the lasing threshold, which prevents the proposed integrator from having an infinite integration time window.

III. EXPERIMENT

The proposed photonic temporal integrator is fabricated in an InP-InGaAsP material system by the UCSB nanofabrication facility, as shown in Fig. 4(a), which is wire-bonded to a carrier for experimental demonstration, as shown in Fig. 4(b). The chip size is 1 mm × 2 mm, and the comparison of its size

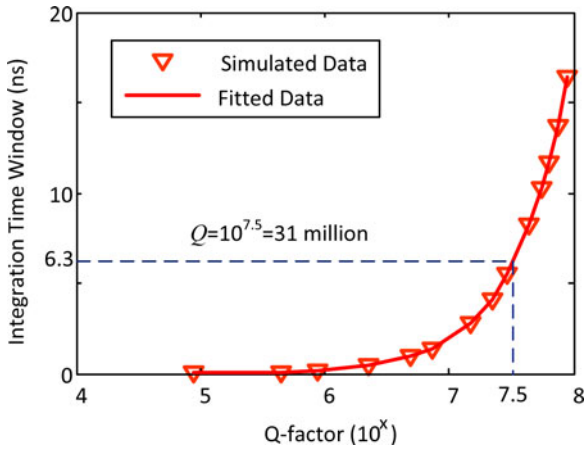

Fig. 3. Simulation results. The integration time window for different Q-factors of the ring.

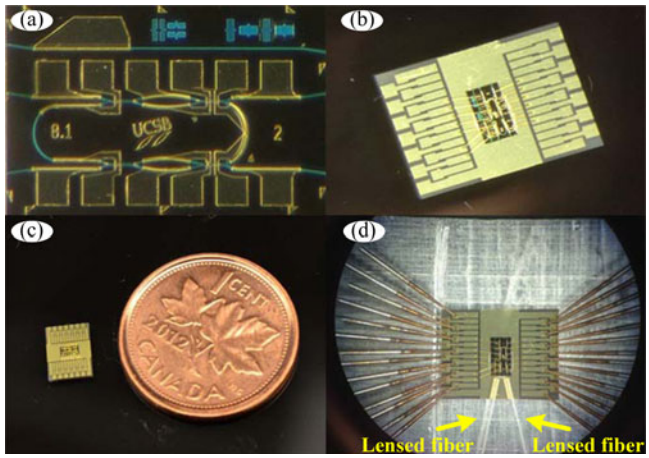

Fig. 4. (a) The fabricated on-chip photonic temporal integrator prototype. (b) Wire bonded to a carrier. (c) Comparison with a Canadian penny. (d) Experimental setup for optical coupling with two lensed fibers.

with a Canadian penny is shown in Fig. 4(c). In the prototype, the length of the deeply etched waveguide ring is 3 mm. Two 400-μm SOAs (SOA02 and SOA03) with a confinement tuning layer offset quantum well [16] structure are fabricated in the ring to provide a peak gain of 9.6 dB per SOA. With 3 mm of ring length subtracting the length of the two SOAs (400 μm each) and 1.7 cm^{-1} of passive waveguide loss, the total waveguide propagation loss is 1.6 dB. For a ring with a coupling coefficient of 90% and 0.5 dB MMI insertion loss, the couplers add about 2 dB of loss for a total round-trip loss of 3.6 dB, which is compensated for by the two SOAs. Two additional active SOAs (SOA01 and SAO04) are incorporated into the system at both the input and output waveguides to compensate for the fiber coupling losses, as shown in Fig. 4(a). In addition, the facets of the waveguides are angled at 7° to minimize the reflections. The phase modulation in the ring and the tuning of the MMI MZI coupler are accomplished by forward bias currents via current injection and free carrier absorption through the carrier

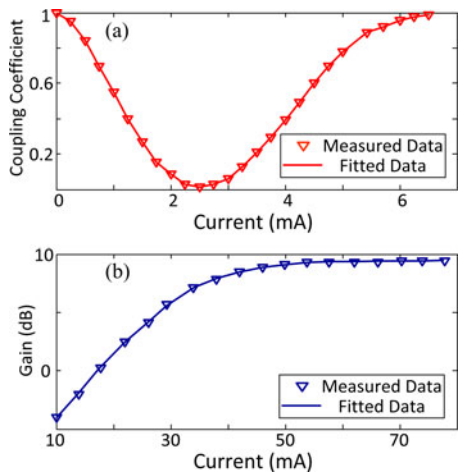

Fig. 5. (a) Tunable coupling coefficient of an MMI MZI coupler at different injection current of one PM on one of the two arms. (b) The gain profile of an SOA as a function of the injection current.

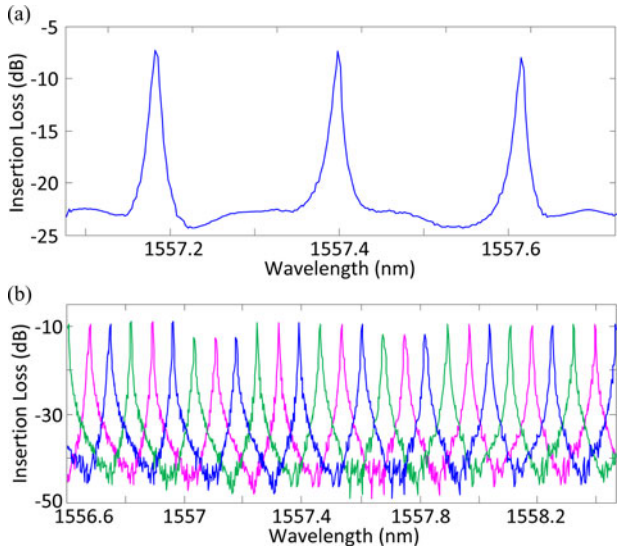

Fig. 6. The measured spectral response of the fabricated ring resonator. (a) The spectral response when no injection current is applied to the PM in the ring. (b) The spectral response of the integrator when the injection current to the PM in the ring is tuned at three different currents.

plasma effect in the PMs. The PMs (PM01-PM05) in the chip are fabricated with a standard length of 300 μm.

The coupling coefficients of the tunable couplers are measured at different injection currents to the PMs, which can be controlled from 0% to 100% when one of the PMs in each of the tunable couplers is injected with a current from 0 to 2.5 mA. Fig. 5(a) shows the measured coupling coefficient of tunable coupler 02 as a function of the injection current to PM02, from 0 to 6.5 mA. The large signal gain profile of an SOA is also measured. As can be seen the SOA has a maximum gain of 9.6 dB when the injection current is above 70 mA, as shown in Fig. 5(b). The FSR of the on-chip ring is measured to be 27.2 GHz as shown in Fig. 6(a). By changing the injection current to the PM (PM05) in the ring, the spectral response of the ring is laterally shifted, thus the peak location is also shifted, as shown in Fig. 6(b). In the experiment, the chip is working at 22 °C with a temperature controlling unit to maximize the stability of the ring resonator.

TABLE II
THE INJECTION CURRENTS TO THE PMS AND SOAS

Components	Integrator	Lasing Condition
SOA01	50.000 mA/2.4992 V	N/A
SOA02	28.300 mA/2.1197 V	39.800 mA/2.3012 V
SOA03	34.202 mA/2.4209 V	34.202 mA/2.4209 V
SOA04	50.000 mA/2.4644 V	N/A
PM01	0	0
PM02	3.7867 mA/1.7758 V	3.7867 mA/1.7758 V
PM03	2.1291 mA/1.7361 V	2.1291 mA/1.7361 V
PM04	0	0

As discussed in Section II, the Q-factor is a critical parameter to the operation of the integrator. In the experiment, we also test the operation of the integrator when it is configured to operate close to the lasing threshold, with the injection currents to the PMs and the SOAs given in Table II. Under this condition of operation, three different input waveforms are generated and applied to the input of the integrator, to study the performance of the integration operation of the device.

A. *Gaussian Pulse*

We first test the integration of a Gaussian pulse by the photonic temporal integrator. The Gaussian pulse is generated by a mode locked laser source which is filtered by an optical bandpass filter (Finisar, WaveShaper 4000 S) with a bandwidth of 0.12 nm and a central wavelength at 1557.4 nm, as shown in Fig. 7(a), to make the Gaussian pulse have a temporal width of 54 ps centered at 1557.4 nm, which is then coupled into the photonic integrator by a lensed fiber. By configuring the photonic temporal integrator with the injection currents to the SOAs and PMs in the ring with the values given in Table II, a high Q-factor of 31 million is achieved and the ring is still under the lasing threshold. As shown in Fig. 7(b), the temporal integral of the input Gaussian pulse is realized. The integration window is measured to be 6331 ps.

B. *In-Phase Doublet*

We then test the integration of an in-phase doublet pulse by the proposed photonic temporal integrator. In the experiment, the in-phase doublet pulse is generated by launching a Gaussian pulse into an unbalanced MZI with a length difference between the two arms of 25 cm. As a result, two closely separated pulses, called an in-phase doublet, with a temporal separation of 1.14 ns, as shown in Fig. 8(a), are generated and then launched into the integrator. The waveform at the output of the integrator is shown in Fig. 8(b). As can be seen the integrator sums up the area of the in-phase doublet, giving two steps corresponding the area of the first pulse and the area of the first and the second pulses, as shown in Fig. 8(b).

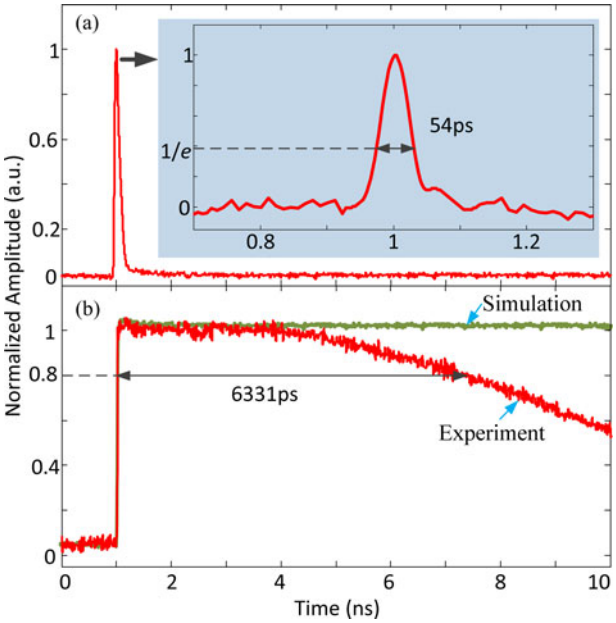

Fig. 7. The experimental results. (a) The input Gaussian pulse with a temporal width of 54 ps. (b) The integral of the Gaussian pulse with an integration time window of 6331 ps.

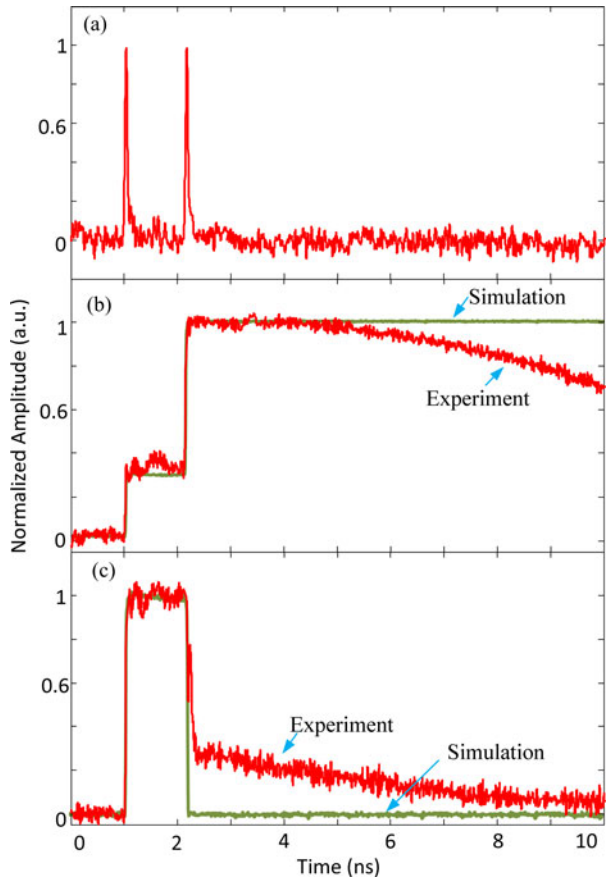

Fig. 8. The experimental results. (a) The input in-phase doublet pulse, (b) the integral of the in-phase doublet pulse, and (c) the integral of the out-of-phase doublet pulse.

C. Out-of-Phase Doublet

A photonic temporal integrator can be used as a memory device. The ability to reset the memory is a very important function. To validate the operation of the integrator as a memory unit, two closely separated pulses with a π phase shift (out-of-phase), called an out-of-phase doublet, generated by the same unbalanced MZI mentioned are coupled into the input port of the integrator. The π phase shift between the two pulses is introduced by the MZI by controlling the length difference between the two arms of the MZI. The waveform at the output of the integrator is shown in Fig. 8(c). As can be seen memory resetting function is performed by the integrator.

IV. Discussion and Conclusion

To utilize the proposed integrator as a processing unit in a large system, the power consumptions of the PMs and SOAs and the amplified spontaneous emission (ASE) noise from the SOAs should be considered. In the experiment, the total power consumption of the integrator is 401 mW including 248 mW consumed by the input/output SOAs, which can be avoided in a large system with all units fabricated on a single chip without fiber coupling loss between the units. In addition, a single SOA in a ring resonator is enough to compensate for the total loss. Therefore, a power consumption with a single SOA in a ring resonator and two PMs for tunable coupling would have a power consumption of 93 mW, which is much smaller than the power consumption of the single integrator demonstrated here. When the number of SOAs is reduced, the ASE noise will also be significantly reduced.

In summary, we have proposed and experimentally demonstrated a fully photonic integrated temporal integrator that provides an ultra-long integration time window and a continuously tunable working wavelength on a single PIC. A temporal integration window of 6331 ps with a bandwidth of 0.12 nm was obtained, which is far better than an electronic integrator. Compared with the previously reported photonic solutions, the proposed integrator provides an integration time window that is an order of magnitude longer. The temporal integration of different input waveforms was also investigated, which confirmed the effective operation of the proposed temporal integrator. This work represents an important step towards the realization of efficient optical signal-processing circuits capable of overcoming the limitation in the integration time window, bandwidth and power consumption imposed by electronics.

References

[1] D. Cotter, R. J. Manning, K. J. Blow, A. D. Ellis, A. E. Kelly, N. Nesset, I. D. Phillips, A. J. Poustie, and D. C. Rogers, "Nonlinear optics for high-speed digital information processing," *Science*, vol. 286, no. 5444, pp. 1523–1528, Nov. 1999.

[2] Y. Ding, X.-B. Zhang, X.-L. Zhang, and D. Huang, "Active microring optical integrator associated with electroabsorption modulators for high speed low light power loadable and erasable optical memory unit," *Opt. Exp.*, vol. 17, no. 15, pp. 12 835–12 848, Jul. 2009.

[3] J. Azana, "Ultrafast analog all-optical signal processors based on fiber-Grating devices," *IEEE Photon. J.*, vol. 2, no. 3, pp. 359–386, Jun. 2010.

[4] Y. Park, T.-J. Ahn, Y. Dai, J. Yao, and J. Azaña, "All-optical temporal integration of ultrafast pulse waveforms," *Opt. Exp.*, vol. 16, no. 22, pp. 17817–17825, Oct. 2008.
[5] M. H. Asghari and J. Azaña, "Design of all-optical high-order temporal integrators based on multiple-phase-shifted Bragg gratings," *Opt. Exp.*, vol. 16, no. 15, pp. 11459–11469, Jul. 2008.
[6] M. H. Asghari and J. Azaña, "On the design of efficient and accurate arbitrary-order temporal optical integrators using fiber Bragg gratings," *J. Lightw. Technol.*, vol. 27, no. 17, pp. 3888–3895, Sep. 2009.
[7] M. H. Asghari, C. Wang, J. Yao, and J. Azaña, "High-order passive photonic temporal integrators," *Opt. Lett.*, vol. 35, no. 8, pp. 1191–1193, Apr. 2010.
[8] Y. Park and J. Azaña, "Ultrafast photonic intensity integrator," *Opt. Lett.*, vol. 34, no. 8, pp. 1156–1158, Apr. 2009.
[9] R. Slavík, Y. Park, N. Ayotte, S. Doucet, T.-J. Ahn, S. LaRochelle, and J. Azaña, "Photonics temporal integrator for all-optical computing," *Opt. Exp.*, vol. 16, no. 22, pp. 18202–18214, Oct. 2008.
[10] M. Ferrera, Y. Park, L. Razzari, B. E. Little, S. T. Chu, R. Morandotti, D. J. Moss, and J. Azaña, "On-chip CMOS-compatible all-optical integrator," *Nature Commun.*, vol. 1, no. 29, pp. 1–5, Jun. 2010.
[11] M. Ferrera, Y. Park, L. Razzari, B. E. Little, S. T. Chu, R. Morandotti, D. J. Moss, and J. Azaña, "All-optical 1st and 2nd order integration on a chip," *Opt. Exp.*, vol. 19, no. 23, pp. 23153–23161, Nov. 2011.
[12] W. Liu, M. Li, R. S. Guzzon, E. J. Norberg, J. S. Parker, L. A. Coldren, and J. P. Yao, "A microwave photonic temporal integrator based on an InP-InGaAsP integrated tunable coupled ring," presented at the IEEE Int. Topical Meeting Microwave Photonics, Alexandria, VA, USA, Oct. 28–31, 2013.
[13] N. Q. Ngo, "Optical integrator for optical dark soliton detection and pulse shaping," *Appl. Opt.*, vol. 45, no. 26, pp. 6785–6791, Sep. 2006.
[14] D. G. Rabus, *Integrated Ring Resonators: The Compendium*, 1st ed. New York, NY, USA: Springer, 2007.
[15] J. Heebner, R. Grover, and T. Ibrahim, *Titre Optical Microresonators: Theory, Fabrication, and Applications,* Series Springer Series in Optical Sciences, vol. 138. New York, NY, USA: Springer, 2008.
[16] E. J. Norberg, R. S. Guzzon, J. S. Parker, S. P. DenBaars, and L. A. Coldren, "An InGaAsP/InP integration platform with low loss deeply etched waveguides and record SOA RF-linearity," in *Proc. 37th Eur. Conf. Exhib. Opt. Commun.*, 2011, pp. 18–22.

Weilin Liu (S'10) received the B.Eng. degree in electronic information engineering from the University of Science and Technology of China, Hefei, China, in 2009, and the M.A.Sc. degree in electrical and computer engineering from the School of Electrical Engineering and Computer Science, University of Ottawa, Ottawa, ON, Canada, in 2011. He is currently working toward the Ph.D. degree and working in the Microwave Photonics Research Laboratory, School of Electrical Engineering and Computer Science, University of Ottawa, Ottawa.

His research interests include microwave/terahertz generation, optical signal processing, fiber Bragg grating and their applications in microwave photonic systems.

Ming Li (S'08–M'09) received the Ph.D. degree in electrical and electronics engineering from the University of Shizuoka, Hamamatsu, Japan, in 2009.

In April 2009, he joined the Microwave Photonics Research Laboratory, School of Electrical Engineering and Computer Science, University of Ottawa, Ottawa, ON, Canada, as a Postdoctoral Research Fellow. In June 2011, he joined the Ultrafast Optical Processing Group, INRS-EMT, Montreal, QC, Canada, as a Postdoctoral Research Fellow. In February 2013, he successfully received a high-level government-funded program ("Thousand Young Talents" program) in China. And then, he joined in the Institute of Semiconductor, Chinese Academy of Sciences as a Full Professor. He has published more than 110 international conference and top-level journal papers. His current research interests include advanced fiber Bragg gratings and their applications to microwave photonics, ultrafast optical signal processing, arbitrary waveform generation, and optical MEMS sensing.

Robert S. Guzzon received the Ph.D. degree in electrical engineering from the University of California at Santa Barbara, Santa Barbara, CA, USA, in 2011 (where this study was performed). There, he developed high dynamic range photonic integrated microwave filter systems, and investigated the spurious free dynamic range of amplified optical systems. He is currently at Aurrion, Inc. in Goleta, CA on silicon photonic systems.

Erik J. Norberg received the Ph.D. degree in electrical engineering from the University of California at Santa Barbara (UCSB), Santa Barbara, CA, USA, in 2011 (where this study was performed). At UCSB, he developed integrated photonic microwave filters and a high dynamic range integration platform on InP. He is an author/coauthor on more than 30 papers.

He is currently an Optoelectronic Design Engineer at Aurrion Inc., Goleta, CA, USA.

John S. Parker received the Ph.D. degree in electrical engineering from the University of California at Santa Barbara, Santa Barbara, CA, USA, in 2012 (where this study was performed). At UCSB, he developed integrated photonic frequency combs with optical phase-locked loops for sensing and coherent communication. He is currently a Photonic Device Scientist at Freedom Photonics in Santa Barbara.

Larry A. Coldren (S'67–M'72–SM'77–F'82–LF'12) received the Ph.D. degree in electrical engineering from Stanford University, Stanford, CA, USA, in 1972.

He is currently the Fred Kavli Professor of optoelectronics and sensors with the University of California at Santa Barbara (UCSB), Santa Barbara, CA. He spent 13 years in research with Bell Laboratories prior to joining UCSB, in 1984, where he holds appointments in electrical and computer engineering and materials. He cofounded Optical Concepts (acquired as Gore Photonics), to develop novel vertical-cavity surface-emitting laser (VCSEL) technology, and later Agility Communications (acquired by JDSU), to develop widely tunable integrated transmitters. With Bell Laboratories, he was involved with surface acoustic wave filters and tunable coupled-cavity lasers using novel reactive ion etching technology. With UCSB, he has continued his involvement on multiple-section lasers, in 1988 inventing the widely tunable multielement mirror concept that is now used in numerous commercial products. He has also made seminal contributions to efficient VCSEL designs. His group continues efforts on high-performance InP-based PICs and high-speed VCSELs. He has authored or coauthored more than 1000 journal and conference papers, a number of book chapters, and a textbook. He holds 64 patents.

Dr. Coldren is a Fellow of Optical Society of America and the Institution of Electrical Engineers. He is a member of the National Academy of Engineering. He received the 2004 John Tyndall Award and 2009 Aron Kressel Award.

Jianping Yao (M'99–SM'01–F'12) received the Ph.D. degree in electrical engineering from the Université de Toulon, Toulon, France, in December 1997. He joined the School of Electrical Engineering and Computer Science, University of Ottawa, Ottawa, ON, Canada, as an Assistant Professor in 2001, where he became an Associate Professor in 2003 and a Full Professor in 2006. He was appointed the University Research Chair in Microwave Photonics in 2007. From July 2007 to June 2010, he was the Director of the Ottawa-Carleton Institute for Electrical and Computer Engineering. Prior to joining the University of Ottawa, he was an Assistant Professor in the School of Electrical and Electronic Engineering, Nanyang Technological University, Singapore, from 1999 to 2001.

He has published more than 450 papers, including more than 260 papers in peer-reviewed journals and 190 papers in conference proceedings. He served as a guest editor for the Focus Issue on Microwave Photonics in Optics Express in 2013. He is currently a Topical Editor for *Optics Letters*, and serves on the editorial board of the IEEE TRANSACTIONS ON MICROWAVE THEORY AND TECHNIQUES. He is a Chair of numerous international conferences, symposia, and workshops, including the Vice-TPC Chair of the 2007 IEEE Microwave Photonics Conference, TPC Co-Chair of the 2009 and 2010 Asia-Pacific Microwave Photonics Conferences, TPC Chair of the high-speed and broadband wireless technologies subcommittee of the 2009–2012 IEEE Radio Wireless Symposia, TPC Chair of the microwave photonics subcommittee of the 2009 IEEE Photonics Society Annual Meeting, TPC Chair of the 2010 IEEE Microwave Photonics Conference, and the General Co-Chair of the 2011 IEEE Microwave Photonics Conference. He received the 2005 International Creative Research Award at the University of Ottawa. He received the 2007 George S. Glinski Award for Excellence in Research. He was selected to receive an inaugural Optical Society of America (OSA) Outstanding Reviewer Award in 2012. He serves as an IEEE Distinguished Microwave Lecturer for 2013–2015.

Dr. Yao is a Registered Professional Engineer of Ontario. He is a Fellow of the OSA, and a Fellow of the Canadian Academy of Engineering.